Supplementary information

Table S1 REAGENT or RESOURCE

REAGENT or RESOURCE	SOURCE	IDENTIFIER
Antibodies		
rabbit anti-UBE2L3	GeneTex	Cat#: GTX104717
mouse anti-human IL-1β	R&D	Cat#: MAB201
goat anti-mouse IL-1β	R&D	Cat#: AF401-NA
rabbit anti-*β*-actin	CST	Cat#:4970S
rabbit anti-STAT3	CST	Cat#:124H6
rabbit anti-pSTAT3	CST	Cat#:9131
mouse anti-mouse CD11c	Abcam	Cat#: ab11029
rabbit anti-human/mouse Ki-67	Abcam	Cat#: ab15580
rabbit anti-K14	Abcam	Cat#: ab181595
rabbit anti-Loricrin	Proteintech	Cat#:55439-1-AP
mouse anti-cytokeratin 1/10	Santa Cruz	Cat#: LH1
Brilliant Violet 510 anti-mouse CD45	Biolegend	Cat#: 157219
FITC anti-mouse I-A/I-E	Biolegend	Cat#:107606
Brilliant Violet 421 anti-mouse CD11c	BD	Cat#:562782
PE/Dazzle™ 594 anti-mouse/ human CD207	Biolegend	Cat#:144212
PE-CY7 anti-mouse CD103	Biolegend	Cat#:121426
efluor660 anti-mouse IL23p19	ThermoFisher	Cat#:50-7023-82
Brilliant Violet 650 anti-mouse TNFα	Biolegend	Cat#:506333
FITC anti-mouse CD3	Biolegend	Cat#:100204

PerCP/Cyanine5.5 anti-mouse CD4	Biolegend	Cat#:100434
APC anti-mouse CD8	BD	Cat#:553035
PE anti-mouse TCRγδ	Biolegend	Cat#:118108
PE-CY7 anti-mouse IL-17A	Biolegend	Cat#:506922
PE anti-mouse CXCL16	BD	Cat#:566740
APC/Cyanine7 anti-mouse CXCR6	Biolegend	Cat#:151124
PE anti-mouse TCR Vγ2	Biolegend	Cat#: 137705
APC anti-mouse TCR Vγ2	Biolegend	Cat#: 137707
FITC Hamster Anti-Mouse Vγ 3 TCR	BD	Cat#: 110067
APC anti-mouse Ki-67	Biolegend	Cat#:652406
Brilliant Violet 510 anti-human CD45	Biolegend	Cat#:368526
APC/Fire™ 750 anti-human HLA-DR	Biolegend	Cat#:327024
FITC anti-human CD3	Biolegend	Cat#:300440
PE/Cyanine7 anti-human CD4	Biolegend	Cat#:357410
APC anti-human CD8	BD	Cat#:570892
PE anti-human IL-17A	Biolegend	Cat#:512306
Brilliant Violet 785 anti-human TNFα	Biolegend	Cat#:502948
BV421 anti-human CD11c	BD	Cat#:566877
eFluor 660 anti-human IL-23p19	eBioscience	Cat#:50-7023-82
PE anti-human CXCL16	Biolgend	Cat#:360803
PE/Cyanine7 anti-human CD186 (CXCR6)	Biolegend	Cat#:356011
PerCP/Cyanine5.5 anti-human CD186 (CXCR6)	Biolegend	Cat#:356009

Rabbit Anti-CD31 antibody	abcam	Cat#: ab182981
Chemicals and recombinant proteins		
Dispase II	Gibco	Cat#: 17105041
Protease and Phosphatase Inhibitor Single-Use Cocktail （100x）	Thermo Fisher	Cat#: 78442
EpiGRO™ Human Epidermal Keratinocyte Complete Culture Media Kit	Millipore	Cat#: SCMK001
FBS	Gibco	Cat#: 10270-106
Trypsin	Gibco	Cat#: T4424
Colleagen IV	Sigma	Cat#:C5533
RPMI medium 1640	Gibco	Cat#: 21875-034
Penicillin-Streptomycin	Gibco	Cat#: 15140122
Tris	Sigma	Cat#: 252859
Sodium Chloride (NaCl)	Sigma	Cat#: S5886
Hanks	Cienry	Cat#:24020
Foxp3 / Transcription Factor Fixation/Permeabilization Concentrate and Diluent	invitrogen	Cat#: 2220751
ELISA MAX™ Deluxe Set Mouse IL-17A	Biolgend	Cat#:432504
Human CXCL16 ELISA kit	Finetest	Cat#:EH0105
Mouse CXCL16 ELISA kit	FineTest	Cat#: EM0005
Recombinant protein human CXCL16	SinoBiological	Cat#: 10834-H08H
Recombinant protein mouse IL-23 protein	SinoBiological	Cat#: CT028-M08H
Recombinant protein mouse CXCL16 protein	Sino Biological	Cat#: 50591-M08H

Recombinant protein mouse IL-17A	Novoprotein	Cat#:CX14
Recombinant protein mouse IL-1β	Novoprotein	Cat#:C042
Recombinant protein human IL-17A	PeproTech	Cat#:20017
Recombinant protein human IL-1beta	PeproTech	Cat#: 200-01B
Human/ mouse Luminex Discovery Assay	BD	no Cat#
Mouse CXCL16 Antibody	R&D	Cat#:AF503
InVivoMAb anti-mouse Vγ2 TCR	Bioxcell	Cat#:BE0168
InVivoMAb polyclonal Armenian hamster IgG	Bioxcell	Cat#:BE0091
InVivoPlus anti-mouse/rat IL-17A	Bioxcell	Cat#:BP0173
InVivoPlus mouse IgG1 isotype control	Bioxcell	Cat#:BP0083
Deposited data		
Raw data files for bulk RNA sequencing: Epidermis and dermis in mouse	This paper	Submitting
Raw data files for single cell RNA sequencing:mouse	This paper	Submitting
Raw data files for single cell RNA sequencing:human	This paper	Submitting
Experimental models: Organisms/strains	SOURCE	IDENTIFIER
C57BL/6	SLAC Laboratory Animal Co.	N/A
Zbtb46-DTR mice	Jackson Laboratories	N/A

Ube2l3fl/fl	Cyagen	N/A
K14-CreERT	Jackson Laboratories	N/A
Rag1-/-	GemPharmatech	N/A
Software and algorithms		
GraphPad v9-10	GraphPad Software	https://www.graphpad.com
ImageJ v1.51	National Institutes of Health (NIH)	https://imagej.nih.gov
GSEA v4.1.0	Subramanian, Tamayo, et al. [49] and Mootha, Lindgren, et al. [50]	http://www.gsea-msigdb.org
R(versions 3.0.0, 4.0.3 and 4.1.3)	The R Foundation	https://www.r-project.org
Cellranger v3.0.2 10x	10x Genomics	https://www.10xgenomics.com/support
Seurat 2.3.0/3.0	The R Foundation	https://satijalab.org/seurat
Harmony	The R Foundation	https://github.com/pardeike/HarmonyLun
SCENIC 1.1.2-2	The R Foundation	https://github.com/aertslab/SCENIC
Metascape v3.5	The R Foundation	http://metascape.org/
Cellchat	The R Foundation	https://www.cellchat..org/

Scrublet	The R Foundation	https://github.com/AllonKleinLab/scrublet
Clusterprofiler v 3.12	The R Foundation	https://bioconductor.org/packages/release/bioc/html/clusterProfiler.html
CellphonDB V2	The R Foundation	https://github.com/ventolab/CellphoneDB?tab=readme-ov-file
CytExpert Software	Beckman Coulter	https://www.mybeckman.cn/flow-cytometry/research-flow-cytometers/cytoflex/software
Photoshop	Adobe	https://www.adobe.com/products/photoshop
Metascape	Zhou et al[24]	https://metascape.org/gp/index.html#/main/step1

Bulk RNA-seq samples collection and data analysis

After sample's RNA extraction and detection were done, library construction and quality control were mad by Illumina's NEBNext® UltraTM RNA Library Prep Kit. Then, the different libraries were subjected to Illumina sequencing.

For quality control, the sequence was verified by fastp software (https://github.com/OpenGene/fastp). HISAT2 (v2.0.5) was used to map reads to the mus musculus. StringTie (https://ccb.jhu.edu/software/stringtie) was used to assemble the mapped reads of each sample. To estimate the expression levels of all transcripts, StringTie and ballgown (http://www.bioconductor.org/packages/release/bioc/html/ballgown.html) were used after the final transcriptome was generated. FPKM (fragment per kilobase of transcript per million mapped reads) value was calculated by StringTie and Ballgown to perform mRNAs expression abundance.

Differential expression analysis between two comparison combinations was performed using DESeq2 software (1.16.1). In mouse epidermal and dermal RNA-

seq, we took the P value <0.05 as well as |log2foldchange|>1.5 as the thresholds for significant differences. Finally, significant up- and down-regulated genes were derived. The GO enrichment analysis of differentially expressed genes was realized by clusterProfiler R software, and the GO term with corrected P-value less than 0.05 was taken as the GO term for significant enrichment of differentially expressed genes. and other high-throughput databases to understand the high-level functions and utility of biological systems such as cells, organisms, and ecosystems. We used clusterProfiler R software to analyze the statistical enrichment of differentially expressed genes in the KEGG pathway. In this paper, metascape (https:/ /metascape. org/gp/index.html#/main/step1) was used to analyze the enrichment of up-regulated significantly differentially analyzed genes. Finally, the enriched pathways were displayed using the visualization tool provided on the website. We used a local version of the Gene Set Enrichment Analysis (GSEA) analysis tool (http://www. broadinstitute. org/gsea/index.jsp) to perform GSEA analyses on the GO, KEGG, and Reactome datasets of this species, respectively. Sequencing data from RNA-seq of mouse epidermis and dermis were subjected to ImmuneCellAI-mouse (http://bioinfo.life.hust.edu.cn/ImmuCellAI-mouse/#! /) deconvolution to perform immune infiltration.

Human/ mouse Luminex Discovery Assay

A custom-made Luminex® assay (LXSAHM; R&D Systems, Minneapolis, Minnesota, USA) was used to detect human and mouse cytokines and chemokines according to the manufacturer's protocol. Briefly, reagents were prepared as instructed. Tissue lysates were made by a RIPA buffer containing protease inhibitors and diluted 1:1 and incubated with the microparticle cocktail at RT for 2 h on a shaker at 800 rpm. Next, wells were washed 3× with wash buffer before incubation with biotin–antibody cocktail for 1h at RT on a shaker at 800 rpm. Subsequently, wells were washed 3× with wash buffer and streptavidin-PE added for 30 min at RT. Wells

were then washed 3× with wash buffer and diluted in wash buffer until reading with the Bio-Plex 200 analyzer (BIO-RAD, Hercules, California, USA) within 60 min.

Western blotting analysis

Cells were lysed with RIPA buffer and lysates were boiled with 5 ×Loading buffer at 95℃ for 10 minutes. Then, the samples were separated with SDS-PAGE gel and immunoblotted with the indicated antibodies. Supernatants of cells were collected and proteins were concentrated by centrifugal concentrators (Millipore). Densitometric analyses were performed using Gel-Pro Analyzer software V4.0 (Media Cybernetics, Bethesda, MD, USA).

Immunofluorescence (IF) and immunohistochemistry (IHC) analyses

In brief, cells were plated on coverslips in 12-well cultured plates, followed by 4% paraformaldehyde solution in PBS for 15 minutes. After washed by PBS, cells were treated with PBS containing 0.3% triton-X100 for 3 mins. Then, cells were washed again and treated with 10% goat blocking serum for 60 mins. After that, cells were primed with primary antibody followed by incubation with corresponding secondary antibody with Alexa Fluor 488 or 555 (Invitrogen). Nuclei were counterstained with DAPI mounting medium. IF assay was captured by fluorescence microscope (Leica DM5500B).

Haematoxylin and eosin (H&E) staining

Skin biopsies were fixed in 10% neutral-buffered formalin and then paraffined. The 4 μm sections were stained with hematoxylin and eosin.

Supplementary Figure Legends

Fig.S1

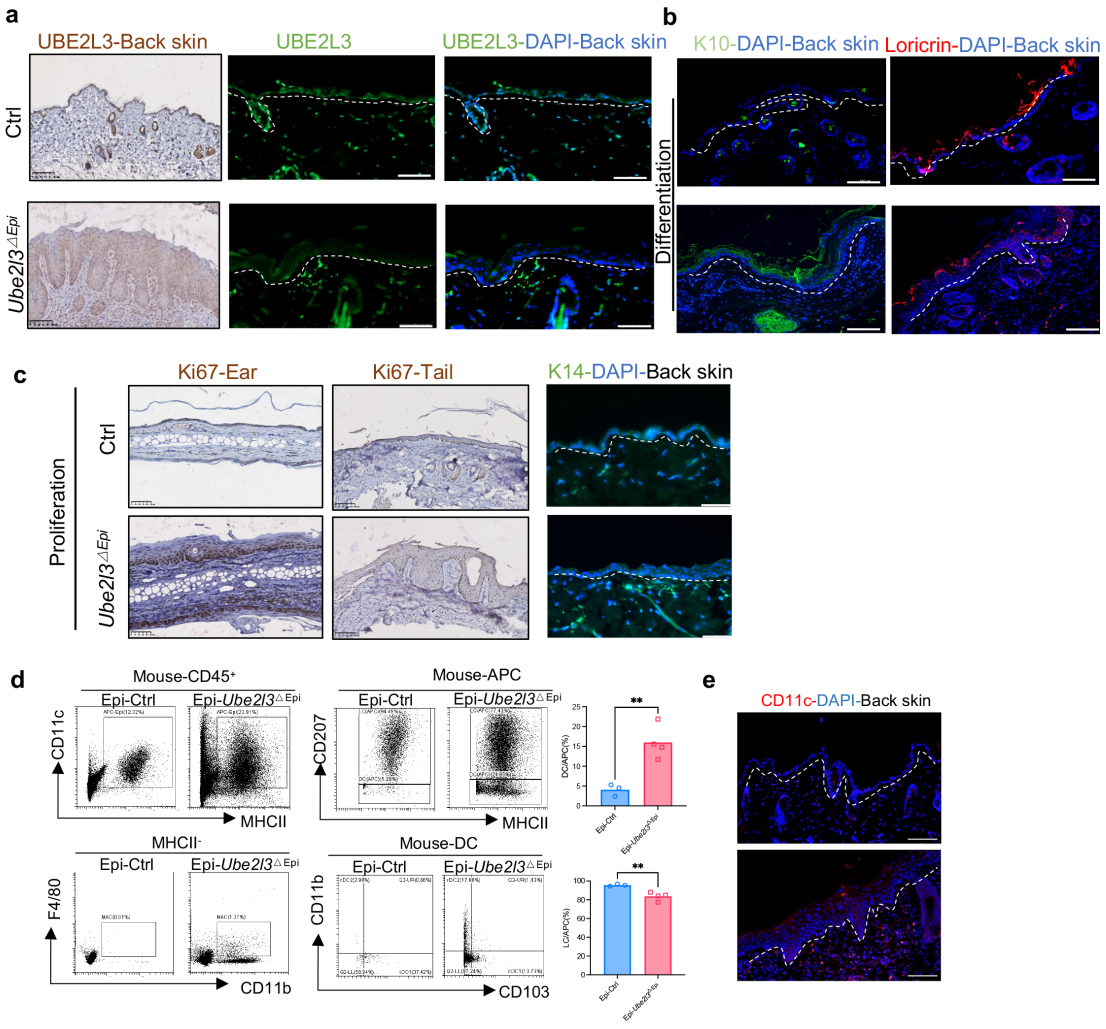

Fig.S1. Spontaneous psoriasis-like dermatitis was detected in *Ube2l3*$^{\Delta Epi}$ mice.

(a)The immunochemistry and immunofluorescence of UBE2L3 in *Ube2l3*$^{\Delta Epi}$ mice and ctrl mice (scale bar= 50μm). (b)The immunochemistry staining of K10 and Loricrin in the skin, ear and nails of *Ube2l3*$^{\Delta Epi}$ mice and ctrl mice (scale bar=100μm). (c) Comparison of proliferation marker (Ki-67) and basal cells ($K14^+$) by immunochemistry and immunofluorescence staining (scale bar=50μm). (d) Representative flow cytometry plots of $CD45^+$ cells, APC, $MHCII^-$ and DC and quantification of the percentage of APC and DC in epidermal back skin of *Ctrl* and *Ube2l3*$^{\Delta Epi}$ mice. **p<0.001. (e) Comparison of myeloid dendritic cells ($CD11c^+$) in the back skin of *Ctrl* and *Ube2l3*$^{\Delta Epi}$ mice using immunofluorescence (Scale bar=100μm).

Fig.S2

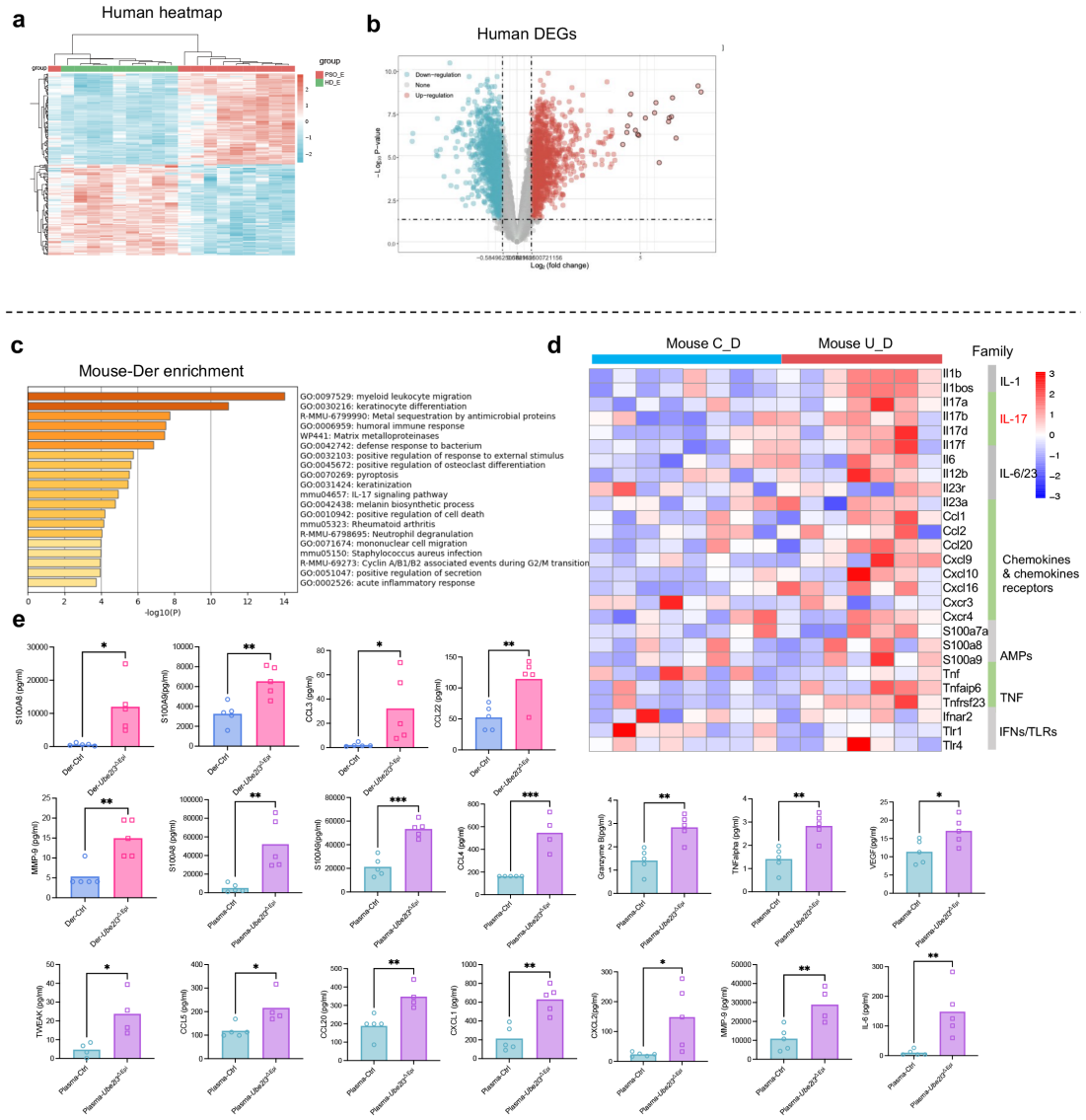
a
Human heatmap
group
P50_E
HD_E
b
Human DEGs
Down−regulation
None
Up−regulation
c
Mouse-Der enrichment
GO:0097529: myeloid leukocyte migration
GO:0030216: keratinocyte differentiation
R-MMU-6799990: Metal sequestration by antimicrobial proteins
GO:0006959: humoral immune response
WP441: Matrix metalloproteinases
GO:0042742: defense response to bacterium
GO:0032103: positive regulation of response to external stimulus
GO:0045672: positive regulation of osteoclast differentiation
GO:0070269: pyroptosis
GO:0031424: keratinization
mmu04657: IL-17 signaling pathway
GO:0042438: melanin biosynthetic process
GO:0010942: positive regulation of cell death
mmu05323: Rheumatoid arthritis
R-MMU-6798695: Neutrophil degranulation
GO:0071674: mononuclear cell migration
mmu05150: Staphylococcus aureus infection
R-MMU-69273: Cyclin A/B1/B2 associated events during G2/M transition
GO:0051047: positive regulation of secretion
GO:0002526: acute inflammatory response
-log10(P)
d
Mouse C_D
Mouse U_D
Family
Il1b
Il1bos
Il17a
Il17b
Il17d
Il17f
Il6
Il12b
Il23r
Il23a
Ccl1
Ccl2
Ccl20
Cxcl9
Cxcl10
Cxcl16
Cxcr3
Cxcr4
S100a7a
S100a8
S100a9
Tnf
Tnfaip6
Tnfrsf23
Ifnar2
Tlr1
Tlr4
IL-1
IL-17
IL-6/23
Chemokines & chemokines receptors
AMPs
TNF
IFNs/TLRs
e
S100A8 (pg/ml)
S100A9(pg/ml)
CCL3 (pg/ml)
CCL22 (pg/ml)
MMP-9 (pg/ml)
S100A8 (pg/ml)
S100A9(pg/ml)
CCL4 (pg/ml)
Granzyme B(pg/ml)
TNFalpha (pg/ml)
VEGF (pg/ml)
TWEAK (pg/ml)
CCL5 (pg/ml)
CCL20 (pg/ml)
CXCL1 (pg/ml)
CXCL3(pg/ml)
MMP-9 (pg/ml)
IL-6 (pg/ml)
Der-Ctrl
Der-Ubx203-/-tsi
Plasma-Ctrl
Plasma-Ubx203-/-tsi

Fig. S2 High significance showed in the epidermis of *Ube2l3*$^{\Delta Epi}$ mice rather than dermis.

(a) Heatmap analysis of GSE166388, GSE68937 and GSE68923 in psoriatic epidermis (PSO_E) and healthy donors (HD_E). (b) Different expressed genes (DEGs) were detected using p-val<0.05 and |log2foldchange|>1.5, which is the same as mouse DEGs. (c) Up-regulated genes in the dermis of *Ube2l3*$^{\Delta Epi}$ mice and Ctrl mice were chosen to do metascape enrichment. (d) Heatmap results in FPKM expression of representative cytokine and chemokine families of IL-1, IL-17, IL-6/IL-23, AMPs, TNF, TLRs, as well as IFNRs in the dermis of Ctrl mice (Mouse C_D_ and *Ube2l3*$^{\Delta Epi}$ mice (Mouse U_D). (e) Protein illumina assay results of S100A8, S100A9, CCL13, CCL22 and MMP9 (pg/ml) in the dermis of Ctrl mice (Der-Ctrl) and *Ube2l3*$^{\Delta Epi}$ mice (Der-*Ube2l3*$^{\Delta Epi}$). Der-Ctrl, n=5, Der-*Ube2l3*$^{\Delta Epi}$, n=5. Protein illumina assay results of S100A8, S100A9, CCL4, Granzyme B, TNFalpha, VEGF, TWEAK, CCL5, CCL20, CXCL1, CXCL2, MMP9, IL-6 (pg/ml) in the plasma of Ctrl mice (Plasma-Ctrl) and *Ube2l3*$^{\Delta Epi}$ mice (Plasma-*Ube2l3*$^{\Delta Epi}$). Plasma-Ctrl, n=5, Plasma-*Ube2l3*$^{\Delta Epi}$, n=4 or 5. ***p<0.001, **p<0.01, *p<0.05.

Fig.S3

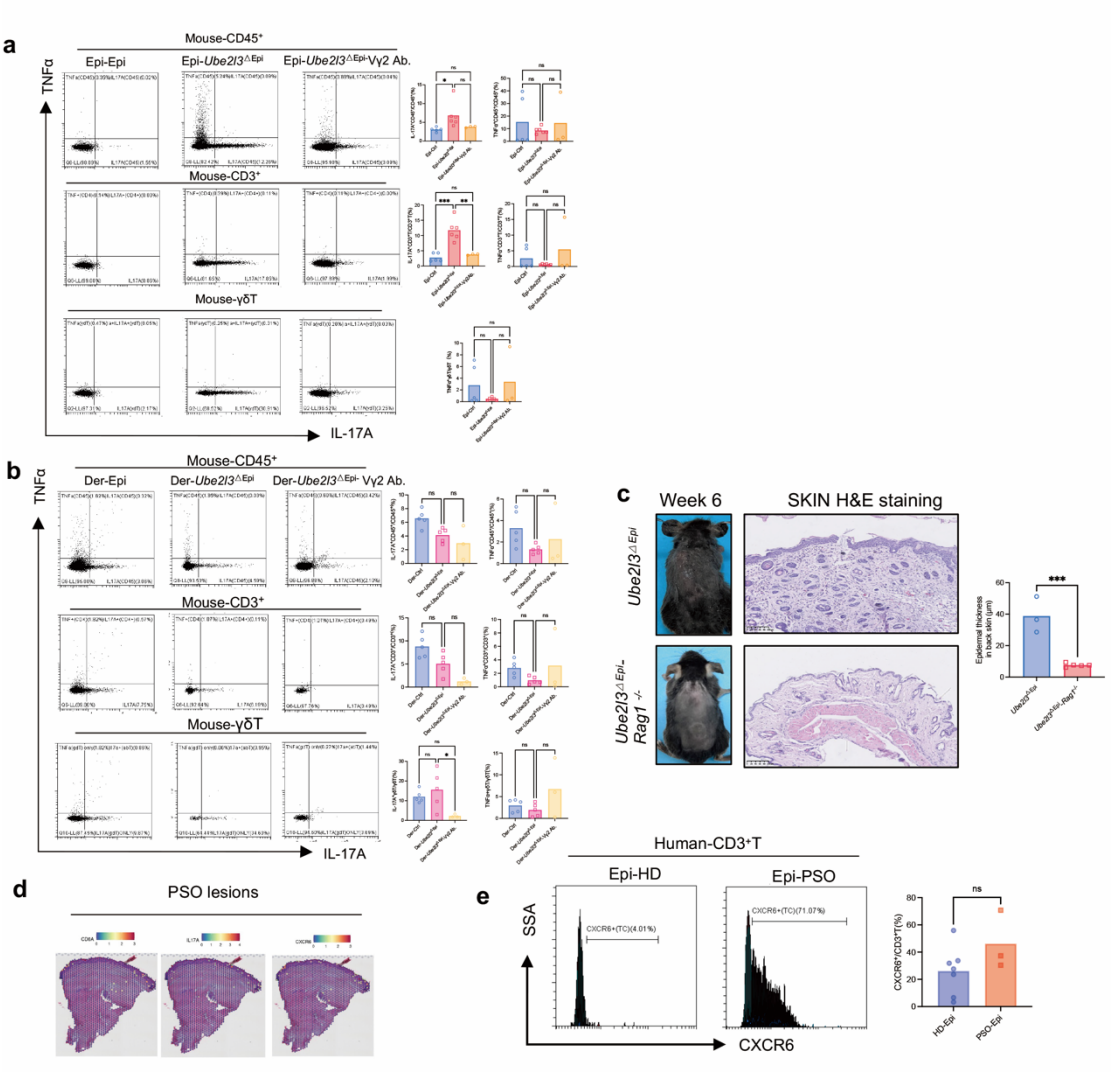

Fig.S3 Mouse dermis lymphocytes subpopulations.

(a) The infiltration score of γδT cells in the epidermis and dermis of Ctrl and *Ube2l3*$^{\Delta Epi}$ mice, used by Immune AI-mouse[51, 52]. (b) Dot plot showing the differentially expressed genes in T cell subsets in healthy adult epidermis, n=2, and psoriatic epidermis, n= 3. (c) Flow cytometry results of percentage of TNFα and IL-17A in the dermis of mouse CD4$^+$T and CD8$^+$T between Ctrl and *Ube2l3*$^{\Delta Epi}$ mice. The bar charts represented Fig.3j and (c) flow cytometric analysis. **， $p<0.01$, ns, not significant. (d) Representative flow cytometric plots in the dermis of mouse control group (Der-Ctrl) and *Ube2l3*$^{\Delta Epi}$ mice (Der-*Ube2l3*$^{\Delta Epi}$). Right bar charts were diiferent proportion of cells in IL-17A$^+$ CD45$^+$ /CD45$^+$ cells, IL-17A$^+$CD3$^+$/CD3$^+$ T cells, IL-17A$^+$αβT/αβT cells, IL-17A$^+$γδT/γδT cells, IL-17A$^+$CD4$^+$/CD4$^+$T cells, IL-

119 $17A^{+}CD8^{+}/CD8^{+}$Tcells, $TNF\alpha^{+}$ $CD45^{+}$/ $CD45^{+}$ cells, $TNF\alpha^{+}$ $CD3^{+}$/ $CD3^{+}$ T cells,
120 $TNF\alpha^{+}\alpha\beta$T/ $\alpha\beta$T cells, $TNF\alpha^{+}\gamma\delta$T/$\gamma\delta$T cells, $TNF^{+}\alpha CD4^{+}/CD4^{+}$T cells, $TNF^{+}\alpha CD8^{+}$/
121 $CD8^{+}$T cells between two groups. **， $p<0.01$, *， $p<0.05$, ns, not significant.

122

Fig.S4

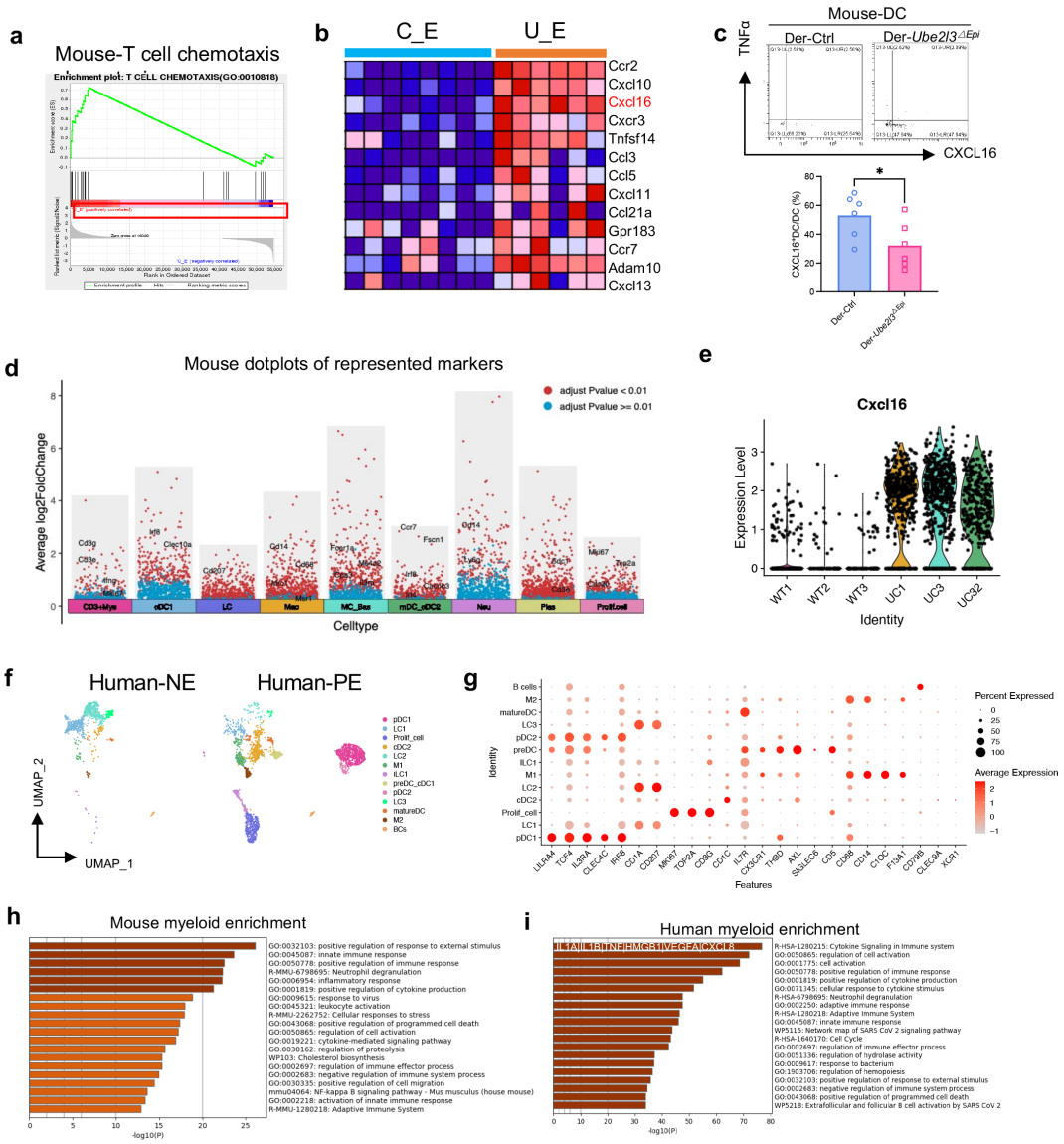

Fig.S4. Epidermal IL-17A^{+}CXCR6^{+}Vγ2^{+}T cells were dominant in the role of psoriasis-like lesion *Ube2l3*$^{\Delta Epi}$ mice

(a) The representative flow cytometric plots and proportion of IL-17A^{+} CD45^{+} /CD45^{+} cells, TNFα^{+} CD45^{+}/ CD45^{+} cells, IL-17A^{+}CD3^{+}/CD3^{+} T cells, TNFα^{+} CD3^{+}/ CD3^{+} T cells, IL-17A^{+}γδT/γδT cells, TNFα^{+}γδT/γδT cells in Epi-Ctrl, Epi-*Ube2l3*$^{\Delta Epi}$, and Epi-*Ube2l3*$^{\Delta Epi-}$ Vγ2Ab groups. ***, $p<0.001$, **, $p<0.01$, ns, not significant.

(b) The representative flow cytometric plots and proportion of IL-17A^{+} CD45^{+} /CD45^{+} cells, TNFα^{+} CD45^{+}/ CD45^{+} cells, IL-17A^{+}CD3^{+}/CD3^{+} T cells, TNFα^{+} CD3^{+}/

$CD3^+$ T cells, IL-$17A^+$γδT/γδT cells, $TNF\alpha^+$γδT/γδT cells in Der-Ctrl, Der-*Ube2l3*$^{\Delta Epi}$, and in dermis of *Ube2l3*$^{\Delta Epi}$ when treated with Vγ2Ab (Der- *Ube2l3*$^{\Delta Epi}$-Vγ2Ab). (c) The experimental procedure of generating *Ube2l3*$^{\Delta Epi}$-*Rag1*$^{-/-}$mice in Mice and ethics of Online methods. Representative images and the H&E staining in the skin of *Ube2l3*$^{\Delta Epi}$-*Rag1*$^{-/-}$mice and *Ube2l3*$^{\Delta Epi}$ mice. scale bar, 100um. ***, $p<0.001$. *Ube2l3*$^{\Delta Epi}$, n=3, *Ube2l3*$^{\Delta Epi}$-*Rag1*$^{-/-}$, n=5.(d) Spatial transcriptomics of CD8A, IL17A and CXCR6 genes in psoriatic lesions in GSE206391. (e) Representative plots and proportion of CXCR6 in $CD3^+$T cells between Epi-HD and Epi-PSO group. ns, not significant. Epi-HD, n=6, Epi-PSO, n=3. Data are presented as means ± S.E.M

Fig.S5

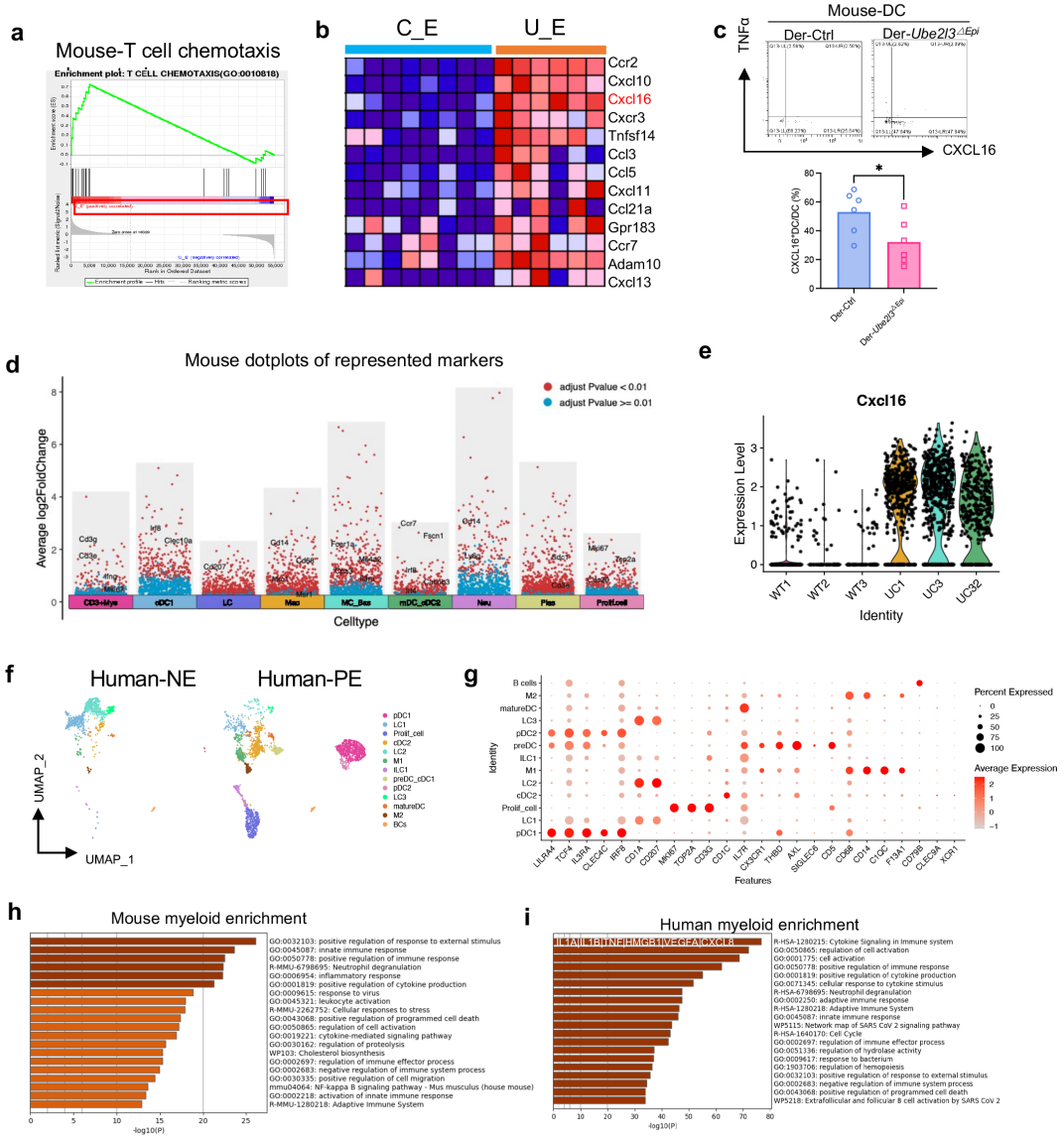

Fig. S5 Similarity of myeloid cells between human psoriasis and mouse psoriasis-like lesion

(a) T cell chemotaxis was increased in U_E group in GSEA of bulk-RNA sequencing. (b) Heatmap showing significantly positive expressed genes in T cell chemotaxis signaling pathway. (c) Representative cytometric plots and percentage of CXCL16 in DC (dendritic cells) in dermis in Der-Ctrl and Der- *Ube2l3*$^{\Delta Epi}$. *， p<0.01. n=6 independent per group. (d) Representative markers used in classifying mouse myeloid

cells. MC_Bas, mast cell and basophils, specified by *Cpa3, Ms4a2* and *Il3ra.* Neu, neutrophils, specified by *Cd14*, *Ly6g*. LC, Langerhans cells, specified by Cd207. Mac, macrophage, specified by *C1qa, C1qb* and *Cd68*. cDC1, type 1 DC, expressed *Xcr1*, *Irf8* and *Clec9a*, less *Irf4*. cDC2, type 2 DC, high expression of Itgam and Irf4, as well as migration marker of *Fscn1*, *Cacnb3*, *Ccr7*. (e)The expression level of Cxcl16 in scRNA-seq in each sample (CE, including WT1, WT2 and WT3, UE, including UC1, UC2, UC32). (f-g) UMAP visualization of all myeloid cells

pDC, specified by *LILRA4, IL3RA, TCF4, CLEC4C*, LC1, LC2, LC3, Langerhans cell cluster1, 2 and 3, specified by *CD207* and *CD1A*. Prolif.T, proliferated associated T cell, specified by *TOP2A, MKI67, CD8A* and *CD3D*. cDC2, type 2 DC, specified by *CLEC10A*, *CD1C* and *ITGAX*. M1, macrophage, specified by *C1QB*, *C1QC*, *M2*, macrophage type 2, specified by *CD68*, *CD14*. ILC1, specified by *IL7R* and low *CD3G*. Pre-DC, specified by *CX3CR1* and *SIGLEC6*. mDC, mature DC, specified by *CCR7, LAMP3*. B cell, specified by CD79A, CD79B[53]. (h-i) Top ten signaling pathway in scRNA-seq of mouse myeloid cell enrichment used by metascape and human myeloid cell enrichment.

References:

1. A. Subramanian *et al.*, Gene set enrichment analysis: a knowledge-based approach for interpreting genome-wide expression profiles. *Proc Natl Acad Sci U S A* **102**, 15545-15550 (2005).
2. V. K. Mootha *et al.*, PGC-1alpha-responsive genes involved in oxidative phosphorylation are coordinately downregulated in human diabetes. *Nat Genet* **34**, 267-273 (2003).
3. Y. Zhou *et al.*, Metascape provides a biologist-oriented resource for the analysis of systems-level datasets. *Nat Commun* **10**, 1523 (2019).
4. Y. R. Miao *et al.*, ImmuCellAI-mouse: a tool for comprehensive prediction of mouse immune cell abundance and immune microenvironment depiction. *Bioinformatics* **38**, 785-791 (2022).
5. Y. R. Miao *et al.*, ImmuCellAI: A Unique Method for Comprehensive T-Cell Subsets Abundance Prediction and its Application in Cancer Immunotherapy. *Adv Sci (Weinh)* **7**, 1902880 (2020).

6. M. Collin, V. Bigley, Human dendritic cell subsets: an update. *Immunology* **154**, 3-20 (2018).